













Research article

Hopanoid distributions differ in mineral soils and peat: a re-evaluation of hopane-based pH proxies

Gordon N. Inglis¹  Cindy De Jonge²  Christoph Häggi³  Sarah J. Feakins³  Jingjing Guo⁴ 
Gerd Dercon⁵  Dailson J. Bertassoli Jr.^{6,7}  Thomas K. Akabane^{7,8}  McKenzie R. Bentley¹ 
Emily Beverly⁹  B. David A. Naafs¹⁰  Richard D. Pancost¹⁰ 

¹ School of Ocean and Earth Science, University of Southampton, Southampton, UK

² Biogeoscience Group, Geological Institute, ETH Zurich, Zurich, Switzerland

³ Department of Earth Sciences, University of Southern California, USA

⁴ Organic Surface Geochemistry Lab, Section 4.6 Geomorphology, GFZ Helmholtz Centre for Geosciences, 14473 Potsdam, Germany

⁵ Soil and Water Management and Crop Nutrition Laboratory, Joint FAO/IAEA Centre of Nuclear Techniques in Food and Agriculture, Department of Nuclear Sciences and Applications, International Atomic Energy Agency, Friedensstrasse 1, 2444 Seibersdorf, Austria

⁶ School of Arts, Sciences and Humanities, University of São Paulo, São Paulo SP, Brazil

⁷ Institute of Geosciences, University of São Paulo, São Paulo SP, Brazil

⁸ University of Bordeaux, CNRS, Bordeaux INP, EPOC, UMR 5805, 33600 Pessac, France

⁹ Department of Earth and Atmospheric Sciences, University of Houston, United States of America

¹⁰ Organic Geochemistry Unit, School of Earth Sciences, School of Chemistry, Cabot Institute for the Environment, University of Bristol, UK

✉ Correspondence to: Gordon Inglis: gordon.inglis@soton.ac.uk

Author contributions: Conceptualization: GNI; Formal analysis: GNI; Funding acquisition: GNI; Investigation: CH, JG, MB; Project administration: GNI; Resources: CDJ, SJF, GD, DJBJ, TKA, EB, BDAN, RDP; Visualization: GNI; Writing – original draft: GNI; Writing – review & editing: GNI, CDJ, CH, SJF, JG, GD, DJBJ, TKA, MB, EB, BDAN, RDP.

Data, code, and outputs: <https://doi.org/10.17605/OSF.IO/3CNJZ>

Submitted: 2025-03-07

Accepted: 2025-06-13

Published: 2025-07-17

Production editor:

Jessica Tierney

Handling editor:

Stephanie Kusch

Reviews:

Darci Rush

One anonymous reviewer

Copyediting:

Anselm Loges,

Marthe Klöcking

Hopanoids are produced by bacteria and are commonly found in terrestrial and marine environments. In modern environments, hopanoids mostly occur in the biological 17 β ,21 β (H) configuration. Over geological time (10⁶ to 10⁸ years), thermal degradation changes their stereochemistry to the thermally mature 17 α ,21 β (H) configuration. However, in modern acidic peat-forming environments, the ‘thermally mature’ C₃₁ 17 α ,21 β (H)-homohopane dominates over the biological $\beta\beta$ stereoisomer, with an increase in the relative abundance of the $\alpha\beta$ stereoisomer at lower pH. Based on this pH dependency, hopane isomerisation ratios have been used to reconstruct pH in ancient peat-forming environments. However, the environmental controls on hopane isomerisation remain poorly constrained and it is unclear whether this proxy is also applicable in mineral soils. Here, we analysed hopane distributions in mineral soils characterised by a wide range of mean annual temperature and pH. We show that mineral soils are dominated by diploptene, an unsaturated C₃₀ hopanoid synthesised by a wide range of bacteria. In our soil dataset, there are relatively few thermally mature $\alpha\beta$ hopanes – even within acidic mineral soils – and there is no relationship between hopane isomerisation ratios and pH. We propose that mineral protection in these soil environments selectively protects hopanoids from rapid degradation and subsequent isomerisation in modern samples. This provides a plausible explanation for the lack of 17 α ,21 β hopanes in modern acidic mineral soil and suggests that the C₃₁ hopane $\beta\beta/(\alpha\beta + \beta\beta)$ index should only be employed as a quantitative pH proxy in peats. Moving forward, we propose that hopane isomerisation ratios can help fingerprint the delivery of (acidic) peat into the marine realm and build upon other biomarker-based proxies developed to trace the input of terrestrial OC into the marine realm.

1 Introduction

Hopanoids are a diverse group of pentacyclic triterpenoids that are abundant in terrestrial and marine environments (Ourisson and Albrecht, 1992; Ries-Kautt and Albrecht, 1989; Rohmer et al., 1984). They are synthesised by a wide variety of bacteria (Talbot et al., 2016) and play a key role in regulating membrane fluidity and permeability (Sáenz et al., 2015). Bacteria synthesise C_{30} hopanoids (diploptene or diplopterol) and/or complex C_{35} bacteriohopanepolyols (BHPs). The latter exhibit a diverse array of side-chain modifications that can be used as tracers for specific bacterial metabolisms (e.g. aerobic methanotrophy, anaerobic ammonium oxidation; Kusch and Rush, 2022). Upon cell death, BHPs undergo a variety of diagenetic transformations, including modification and subsequent loss of the polyfunctionalised side chain. This leads to the formation of various geohopanoids, including hopanes, hopenes, hopanols, and hopanoic acids. With increasing thermal maturation, the biological isomer ($17\beta,21\beta$; $\beta\beta$ hereafter) is transformed into the more stable $17\beta,21\alpha$ ($\beta\alpha$ hereafter) and then $17\alpha,21\beta$ ($\alpha\beta$ hereafter) isomer (Mackenzie et al., 1980). This process normally occurs slowly over timescales of 10^6 – 10^8 years but even ~ 200 -million-year-old claystone and limestone deposits can still contain abundant thermally immature $\beta\beta$ hopanes (Robinson et al., 2017).

Hopane $\beta\beta/(\alpha\beta + \beta\beta)$ indices have been used extensively within the petroleum industry to assess source rock maturity (Farrimond et al., 1998; Mackenzie et al., 1980). However, thermally mature hopanes have also been identified in some contemporary environments that have not undergone thermal maturation. In modern peats, the 'thermally mature' C_{31} $17\alpha,21\beta$ -homohopane (C_{31} $\alpha\beta$ hopane, hereafter) can dominate over the biological $\beta\beta$ isomer (Huang et al., 2015; Inglis et al., 2018; Quirk et al., 1984). The C_{31} $\alpha\beta$ hopane has been detected in surficial peat sediments (< 2 cm), indicating that this transformation occurs quickly, likely within decades (Huang et al., 2015; Inglis et al., 2018). This rapid transformation in peats has been attributed to acid-catalysed isomerisation of the $\beta\beta$ isomer at low pH (Quirk et al., 1984) and there is a significant positive correlation between C_{31} hopane isomerisation and pH ($n = 94$, $r^2 = 0.64$, $p < 0.001$) in a global wetland database (Inglis et al., 2018). The C_{31} hopane $\beta\beta/(\alpha\beta + \beta\beta)$ index has since been used to reconstruct pH (qualitatively or quantitatively) within modern (Schaaff et al., 2024) and ancient (Inglis et al., 2019; Lauretano et al., 2021; Witkowski et al., 2023) peat-forming environments. In these studies, hopane-derived pH estimates are consistent with independently derived branched GDGT-derived pH estimates. However, there is an offset in the carbon isotopic composition ($\delta^{13}C$) of C_{31} $\alpha\beta$ and $\beta\beta$ isomers in some modern tropical peats. For example, in Indonesian (Inglis et al., 2019) and Cameroonian peats (Schaaff et al., 2024) the C_{31} $\beta\beta$ isomer is ^{13}C -depleted (up to 10 ‰) compared to the $\alpha\beta$ isomer, implying that $\alpha\beta$ and $\beta\beta$ isomers in peats may be synthesised de novo by different source organisms with unique metabolic strategies (e.g. heterotrophs vs methanotrophs). If true, this implies

that pH alone is unlikely to explain the dominance of the 'thermally mature' C_{31} $\alpha\beta$ hopane in peat (Schaaff et al., 2024).

If pH is the main driver of this rapid transformation, we hypothesise that acidic mineral soils would also be dominated by $\alpha\beta$ hopanes. To explore whether hopanoids in acidic mineral soils are characterised by similarly rapid isomerisation of the $\beta\beta$ isomer, we present the first global analysis of hopane distributions within modern mineral soils ($n = 102$). Our soil dataset spans a wide range of mean annual temperatures (~ 0 – $26^\circ C$) and pH (3 to 9), allowing us to explore how changes in these environmental parameters influence hopane isomerisation ratios. We then compare C_{31} hopane $\beta\beta/(\alpha\beta + \beta\beta)$ indices in mineral soils (i.e. mineral-rich soils with $< 30\%$ total organic carbon content; Brady and Weil, 2008) and peats (i.e. organic-rich soils developed under anoxic conditions with ~ 30 – 60% total organic carbon content) to re-evaluate the use of hopanoids as pH proxies in modern and ancient terrestrial environments.

2 Methods

2.1 Mineral and soil sampling

To generate a database of hopane and hopene distributions in modern mineral soils, we analysed soil samples ($n = 102$) from elevation gradients that cover a large temperature range over a smaller spatial scale including (i) Austria, Mt. Rauris ($n = 12$; 1050–2050 m a.s.l.; De Jonge et al., 2024); (ii) Bolivia, Mt. Zongo ($n = 8$; 1198–4210 m a.s.l.; De Jonge et al., 2024); (iii) China, Mt. Gongga ($n = 8$; 1915–3788 m a.s.l.; De Jonge et al., 2024); (iv) upland Tanzania, Mt. Kilimanjaro ($n = 8$; 920–3660 m a.s.l.; De Jonge et al., 2024); and sites from lowland Tanzania ($n = 11$; 1100–1700 m a.s.l.; Beverly et al., 2021; Zhang et al., 2021; Peaple et al., 2022) and various locations across Brazil ($n = 41$) and Colombia ($n = 14$; 200–1200 m a.s.l.; Häggi et al., 2023) that encompass a wide range of pH values (see Table S1 in Inglis, 2025).

The mineral soil database spans a wide range of temperatures (~ 0 – $26^\circ C$), pH (3 to 9), stable carbon isotope values (-20.5 to -29.9 ‰) and total organic carbon content (0.6–27.8 wt%; see Table S1). In our dataset, most samples are derived from relatively acidic mineral soils with pH < 5 ($n = 63$). However, the data set includes mineral soils that are moderately acidic to neutral (i.e. pH 5 to 7; $n = 28$), and alkaline (i.e. pH 7 to 9, $n = 11$). Sites are characterised by a range of vegetation, including grasslands, shrubland, savannas, and rainforests. For full details on each site and sampling strategy, see De Jonge et al. (2024), Peaple et al. (2022), and Häggi et al. (2023).

2.2 Data compilation for peats

Mineral soil samples are complemented by published C_{31} hopane $\beta\beta/(\alpha\beta + \beta\beta)$ indices compiled from a global database of peat deposits ($n = 94$ sites; Inglis et al., 2018). We also include unpublished hopane and hopene data from

various peatlands (Inglis et al., 2018), specifically Pinheiros, Brazil (n = 14 samples from 1 site), Bomfield Swamp, Australia (n = 8 from 1 site), Harz, Germany (n = 11 from 1 site), Zalama, Spain (n = 8 from 1 site), Sebangau, Indonesia (n = 8 from 1 site) and various sites across the USA (n = 10 samples from 10 sites) and Peru (n = 37 from 9 sites; see Table S3). These samples (n = 96 samples from 7 countries and 24 unique sites) include surface peats (0–2 cm) and peat cores spanning the upper 100 cm (i.e. acrotelm and catotelm). The acrotelm (0–15 cm; Naafs et al., 2017) is assumed to be oxic whereas the catotelm (15–100 cm; Naafs et al., 2017) is permanently waterlogged and characterised by anoxic conditions (Naafs et al., 2017). The peat samples cover a broad range in mean annual temperature (MAAT) from 1 to 26 °C and are characterised by a wide variety of vegetation, ranging from *Sphagnum*-dominated ombrotrophic peats to *Cyperaceae*-dominated minerotrophic peats. These peats (n = 96) were extracted with an Ethos Ex microwave extraction system using 15 mL of dichloromethane (DCM) and methanol (MeOH; 9:1 by volume) at the Organic Geochemistry Unit in Bristol (Inglis et al., 2018). The TLE was then separated using silica column chromatography into hydrocarbon, aromatic and polar fractions using 100 % hexane, hexane:DCM (3:1 by volume) and DCM:MeOH (1:2 by volume). For full details on each site and the experimental protocol, see Inglis et al. (2018) and Naafs et al. (2017).

2.3 Organic geochemistry

Mineral soil sampled along altitudinal transects in Austria (n = 12), Bolivia (n = 8), China (n = 8) and Tanzania (n = 8) were prepared for analysis at ETH Zurich as described in De Jonge et al. (2024). Briefly, soil was freeze dried, homogenised, and extracted using an energised dispersive guided extraction (EDGE) system using a mixture of dichloromethane (DCM) and methanol (MeOH; 9:1 by volume) at 110 °C. Samples were kept at extraction temperature for 3 minutes, and subsequently flushed twice with the solvent mixture at 110 °C, resulting in a total of three extraction rounds. The total lipid extract (TLE) was subsequently dried under a gentle N₂ stream and separated into hydrocarbon (F1), ketone (F2) and polar (F3) fractions by passing them over an activated Al₂O₃ column using hexane:DCM (9:1 by volume), hexane:DCM (1:1 by volume) and DCM:MeOH (1:1 by volume), respectively. Sediment from sites across Brazil (n = 41), Colombia (n = 14) and low-land Tanzania (n = 11) were extracted using an accelerated solvent extraction system (ASE 350 Accelerated Solvent Extractor) with a 9:1 mixture (by volume) of DCM:MeOH and two 15 minute extraction cycles (100 °C, 1500 psi or 10.34 MPa) at University of Southern California. An aliquot of the total lipid extract (TLE) was then separated at the University of Southampton into hydrocarbon (F1), ketone (F2) and polar (F3) fractions using hexane (100 %), hexane:DCM (3:1 by volume) and DCM:MeOH (1:2 by volume), respectively.

Hydrocarbon fractions (containing hopanes and hopenes; n = 102) were analysed using a ThermoFisher Trace 1310 Gas Chromatograph coupled to a Thermo TSQ8000 Triple Quadrupole MS (GC/MS-MS) at the University of Southampton. Separation was achieved with a DB-5 column (30 mm × 0.25 mm internal diameter, 0.25 µm film thickness). The GC temperature program started at 70 °C for 1 minute, increased to 130 °C at 20 °C min⁻¹, followed by 300 °C at 4 °C min⁻¹, which was then held for 20 minutes. MS scanning occurred between mass-to-charge ratio (*m/z*) 50 to 650 Daltons, and used an ionisation energy of 70 eV. Hopanes and hopenes were identified based upon published mass spectra, characteristic mass fragments and retention times (Moldowan et al., 1991; Sessions et al., 2013; Sinninghe Damsté et al., 2014). Hopanes and hopenes in mineral soils (this study) and peats (Inglis et al., 2018; this study) were integrated using the *m/z* 191 mass fragment.

2.4 Biomarker ratios

The hopane isomerisation ratio is calculated as follows:

$$C_n = \beta\beta / (\alpha\beta + \beta\beta) \quad (1)$$

where *C_n* is the carbon chain length (e.g. *C*₃₁). A lower contribution of ββ isomers is marked by values closer to 0. The relative abundance of diplotene is expressed as a fraction of the total hopanoid assemblage:

$$f_{\text{diplotene}} = \frac{\text{diplotene}}{\sum \text{hopanes} + \sum \text{hopenes}} \quad (2)$$

A higher contribution of diplotene is marked by values closer to 1.

2.5 Statistical analysis

Unconstrained principal component analysis (PCA) was used to visualise the variance in compositional data: (i) within different mineral soils (Fig. 1a) and (ii) between mineral soils and peat (Fig. 2a). Standardised compositional data is mapped into Euclidean space using a centred log-ratio (CLR) transformation (Aitchison, 1986). For mineral soils (Fig. 1), we use the standardised fractional abundances of seven hopanes (17β(H)-trishnorhopane (*C*₂₇); 17β,21α(H)-norhopane (*C*₂₉); 17β,21β(H)-norhopane (*C*₂₉); 17α,21β(H)-hopane (*C*₃₀); 17β,21β(H)-hopane (*C*₃₀); (22R)-17β,21α(H)-homohopane (*C*₃₁); 17β,21β(H)-homohopane (*C*₃₁)) and six hopenes (22,29,30-Trishnorhop-17(21)-ene (*C*₂₇); hop-17(21)-ene (*C*₃₀); neohop-13(18)-ene (*C*₃₀); moretene (*C*₃₀); hop-22(29)-ene [diplotene] (*C*₃₀); hop-21(22)-ene (*C*₃₀)). As peats have a more diverse hopanoid distribution than mineral soils, additional compounds are included in Figure 2 (specifically, an additional unknown *C*₃₀ hopene, 17β,21α(H)-hopane (*C*₃₀), (22S)-17β,21α(H)-homohopane (*C*₃₁), 17,21-epoxyhopane, and 17β,21β(H)-bishomohopane (*C*₃₂)).

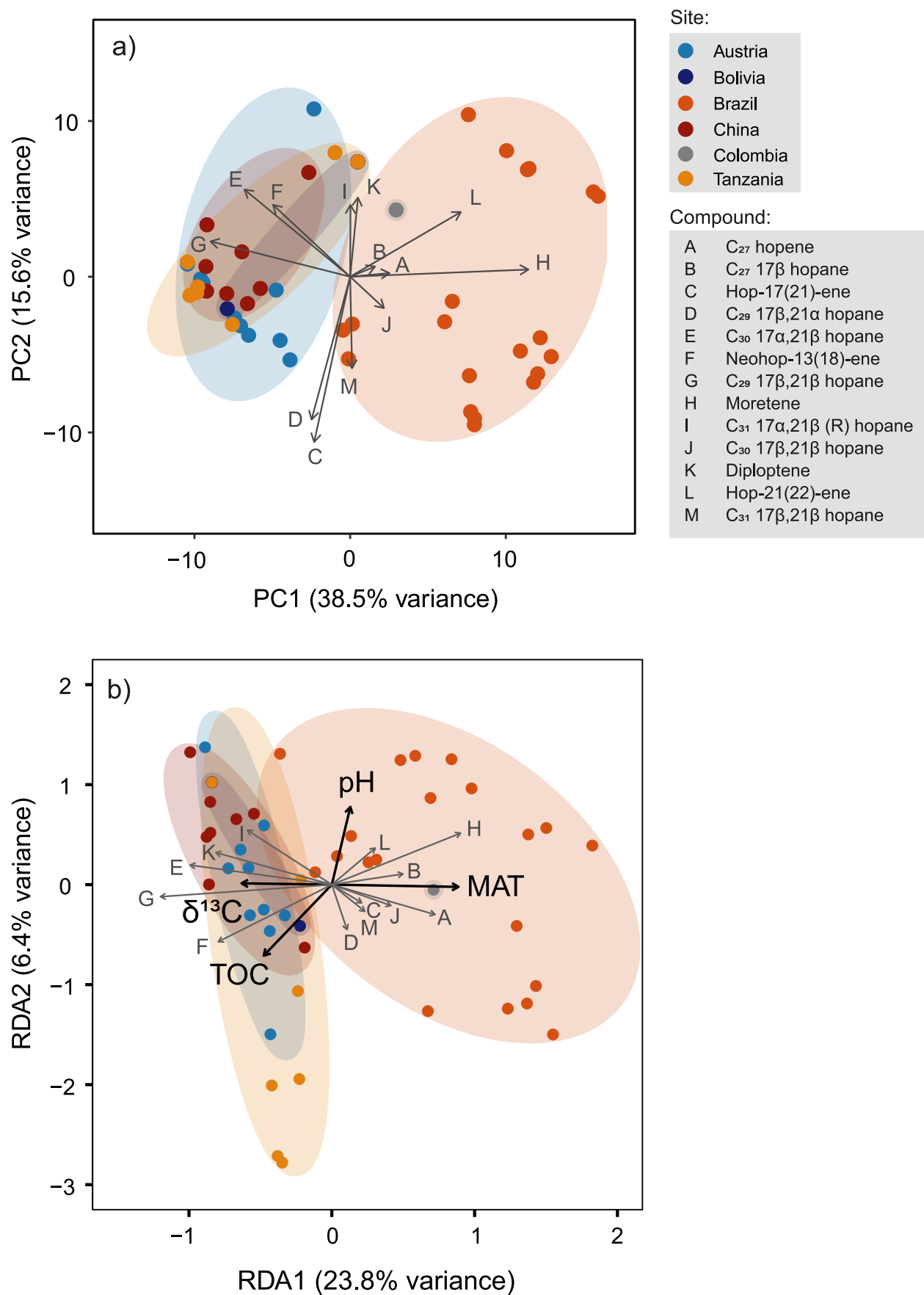


Figure 1. (a) PCA based on standardised fractional abundances of hopanes and hopenes (see key) in modern mineral soils across five different regions (Austria, Brazil, Bolivia, upland Tanzania, China). (b) RDA showing variance of standardised fractional abundances of hopanes and hopenes (see key) explained by environmental variables (pH, MAT (mean annual air temperature), TOC (total organic carbon) and $\delta^{13}\text{C}$). Ellipses represent 68 % confidence intervals.

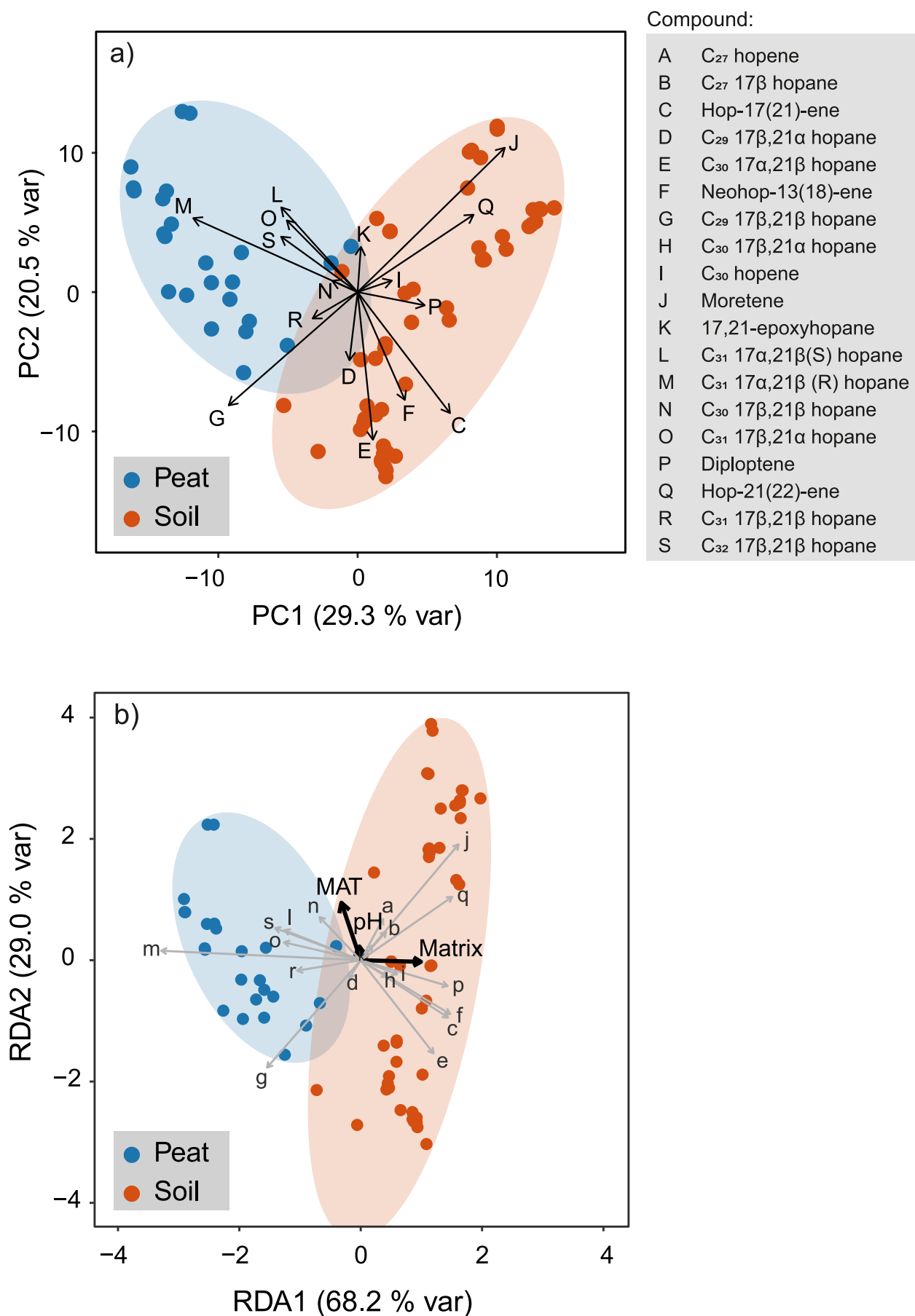


Figure 2. (a) PCA based on standardised fractional abundances of hopanes and hopenes in peat and soil datasets. Compounds (A), (B) and (H) excluded as they are superimposed in the biplot and exhibit relatively low values on PC1 and PC2. (b) RDA showing variance in standardised fractional abundances of hopanes and hopenes explained by environmental variables (pH, mean annual air temperature, and matrix type).

Redundancy analysis (RDA; i.e. a constrained ordination technique) is subsequently used to determine how much variance can be explained by a set of explanatory (i.e. environmental) variables. Environmental variables were obtained from [De Jonge et al. \(2024\)](#), [Häggi et al. \(2023, 2024\)](#) and [Naafs et al. \(2017\)](#). When comparing peat and soil biomarker distributions, their assignment as peat or soil is included as an explanatory factor. PCA and RDA analysis were carried out using RStudio and *dplyr* ([Wickham et al., 2023](#)), *ggplot2* ([Slowikowski, 2024](#)), *scales* ([Wickham et al., 2019](#)), *ggforce* ([Pederson, 2022](#)), *vegan* ([Oksanen et al., 2001](#)) and *compositions* ([van den Boogaart and Tolosana-Delgado, 2008](#)) packages. Ridgeline plots were generated using the *ggridges* package ([Wilke, 2017](#)). Non-parametric *t*-tests were used to determine the statistical difference between datasets.

3.1 Hopanoid distributions in mineral soils and peats

Figure 1 displays three panels (a, b, c) showing the probability density functions (PDFs) for different parameters, comparing Peat (orange) and Soil (blue) distributions. The x-axis for all panels is 'Ratio' (0.00 to 1.00).

a) $f_{\text{diploptene}} (\%)$

Peat distribution (orange) is concentrated at low ratios (0.00 to 0.50), peaking around 0.10. Soil distribution (blue) is concentrated at high ratios (0.50 to 1.00), peaking around 0.80.

b) $C_{31} \beta\beta/(\alpha\beta+\beta\beta)$

Peat distribution (orange) is concentrated at low ratios (0.00 to 0.50), peaking around 0.10. Soil distribution (blue) is concentrated at high ratios (0.50 to 1.00), peaking around 0.90.

c) $\Sigma\text{hopane } \beta\beta/(\alpha\beta+\beta\beta)$

Peat distribution (orange) is concentrated at low ratios (0.00 to 0.50), peaking around 0.30. Soil distribution (blue) is concentrated at high ratios (0.50 to 1.00), peaking around 0.80.

Hopanes and/or hopenes were detected in 51 out of 102 samples (see Table S2). The dominant hopanoid in the hydrocarbon fraction was typically hop-22(29)-ene (diploptene). In a subset of samples, 22,29,30-Trisnorhop-17(21)-ene (C_{27} hopene) or 17 α ,21 β (H)-norhopane (C_{29} $\alpha\beta$ hopane) dominated the hopanoid assemblage. A range of other minor compounds were detected, including: 17 β (H)-trisnorhopane (C_{27}), 17 β ,21 β (H)-norhopane (C_{29}), 17 α ,21 β (H)-, and 17 β ,21 β (H)-hopane (C_{30}), (22R)-17 β ,21 α (H)- and -17 β ,21 β (H)-homohopane (C_{31}), neohop-13(18)-ene, and hop-17(21)-ene (C_{30}).

6

Table 1. Summary of surface mineral soil samples collected ($n = 102$) and the number of samples in which hopanoids (including the C_{31} $\alpha\beta$ hopane and diploptene) were detected.

Country	Surface samples	Hopanoids detected	C_{31} $\alpha\beta$ hopane detected	Diploptene detected
Austria	12	10	0	10
Bolivia	8	4	1	4
Brazil	41	21	0	20
China	8	8	0	8
Colombia	14	1	0	0
Lowland Tanzania	11	0	0	0
Upland Tanzania	8	7	1	7
Total	102	51	2	49

Table 2. Summary of peat samples collected ($n = 96$ from 24 sites) and the number of samples in which hopanoids (including the C_{31} $\alpha\beta$ hopane and diploptene) were detected.

Country	Sites	Samples	Hopanoids detected	C_{31} $\alpha\beta$ hopane detected	Diploptene detected
Australia	1	8	8	8	8
Brazil	1	14	14	14	12
Indonesia	1	8	8	8	8
Spain	1	8	8	8	8
Germany	1	11	11	11	9
Peru	9	37	37	37	37
USA	10	10	10	10	9
Total	24	96	96	96	91

were found under grasslands with some tree cover in the Serengeti ecosystem, perhaps due to the alkaline nature of soils. In Brazil and Colombia, null results were mostly found in soils under grass dominated Cerrado vegetation types (all samples), semi-arid Caatinga shrublands (all samples), and most samples from Llanos riparian forests and Mauritania swamps.

In peats, hopanes and/or hopenes were detected in all samples (Table 2). As reported previously (Inglis et al., 2018), the dominant hopanoid in the hydrocarbon fraction was typically the (22R)-17 α ,21 β (H)-homohopane (C_{31}). However, in some settings 17 β (H)-trisnorhopane (C_{27}), hop-22(29)-ene (C_{30} ; diploptene) or two C_{30} hopenes with unknown structures dominated the hydrocarbon fraction (Table S4).

3.2 Hopanoid ratios in mineral soils and peats

The degree of hopane isomerisation was assessed using $\beta\beta/(\alpha\beta + \beta\beta)$ indices (following Mackenzie et al., 1980). In mineral soils, the C_{31} hopane $\beta\beta/(\alpha\beta + \beta\beta)$ index ranges from 0.64 to 1.00 with an average value of 0.98 ($n = 51$, $\sigma = 0.08$; Figure 4b; Table S2) whereas C_{27} - C_{31} hopane $\beta\beta/(\alpha\beta + \beta\beta)$ indices span a wider range (from 0.28 to 1.00) with an average value of 0.74 ($n = 48$, $\sigma = 0.17$; Figure 4c). In peats, the C_{31} hopane $\beta\beta/(\alpha\beta + \beta\beta)$ indices range from 0.05 to 0.75 with an average value of 0.26 ($n = 24$, $\sigma = 0.21$; Figure 4b; Table S4) whereas C_{27} - C_{31} hopane $\beta\beta/(\alpha\beta + \beta\beta)$ indices span a wider range (from 0.04 to 0.91) with an average value of 0.50 ($n = 24$, $\sigma = 0.22$; Figure 4c).

In mineral soils, diploptene was detected in 49 out of 102 samples. In samples where hopanoids were detected

($n = 51$), the relative abundance of diploptene ($f_{\text{diploptene}}$) is calculated and ranges from 0 to 1 with a mean value of 0.64 ($n = 51$, $\sigma = 0.28$; Figure 4a; Table S2). In peats, diploptene was detected in 91 out of 96 samples. In peat, the relative abundance of diploptene ($f_{\text{diploptene}}$) is lower and ranges from 0.00 to 0.39 with a mean value of 0.11 ($n = 24$, $\sigma = 0.11$; Figure 4a; Table S4).

3.3 PCA and RDA results

In mineral soils, the first two PCA axes account for a cumulative 54 % of the variance (Fig. 1a). Moretene and C_{29} $\beta\beta$ hopane are most strongly associated with PC1, whereas diploptene, C_{31} $\alpha\beta$ hopane and C_{31} $\beta\beta$ hopane are most strongly aligned with PC2 (Fig. 1a). Mineral soils from upland Bolivia, China, Tanzania, and Austria are visually separated from the lowland Brazilian mineral soils. This separation is driven by (i) the absence of moretene and hop-21(22)-ene in upland mineral soils in Austria, Bolivia, China and upland Tanzania and (ii) the absence of C_{29} $\beta\beta$ hopane, C_{30} $\alpha\beta$ hopane and neohop-13(18)-ene in mineral soils from Brazil. In mineral soils, the four environmental variables (MAT, pH, TOC and $\delta^{13}\text{C}$) together explain ~ 34 % of the total constrained variance (Fig. 1b). MAT, pH, and TOC are statistically significant ($p < 0.005$) whereas $\delta^{13}\text{C}$ is not ($p > 0.05$). Approximately 66 % of variation remains unexplained and highlights the potential influence of additional environmental or geochemical factors.

Comparing lipid distributions in mineral soils and peats, the first two PCA axes account for a cumulative 50 % of the variance (Fig. 2a). Peats predominantly lie on the left side of the plot (negative values on PC1) whereas

mineral soils cluster on the right side (positive values on PC1; Fig. 2a). This is largely driven by differences in the relative abundance of C₃₀ hopenes and C₃₁ hopanes (Fig. 2a). Mineral soils are characterised by relatively more C₃₀ hopenes (e.g. diploptene, moretene, hop-17(21)-ene) whereas peats are dominated by the C₃₁ αβ hopane. In the combined dataset MAT and pH are the only available environmental parameters. The RDA analysis shows that MAT, pH and matrix type (a categorical factor that includes whether the sample is mineral soil or peat) together account for ~36 % of the constrained variance (Fig. 2b). MAT and matrix type are both statistically significant ($p < 0.01$) whereas pH is not ($p = 0.266$).

4 Discussion

4.1 Diploptene is the dominant hopanoid in mineral soil hydrocarbon fractions

Diploptene is biosynthesised by a wide variety of bacteria (Rohmer et al., 1984), including heterotrophs, methanotrophs and autotrophs, and is an essential precursor in the formation of BHPs (Bradley et al., 2010). Consistent with this broad range of source organisms, diploptene (or hop-22(29)-ene) is abundant in grassland and forest mineral soils (Ries-Kautt and Albrecht, 1989; Shunthirasingham and Simpson, 2006). However, it is unknown whether this dominance persists across mineral soil types as this assessment is based upon a small number of samples ($n = 8$) from only two localities (Canada and France). Our expanded mineral soil dataset confirms that when hopanoids are detected ($n = 51$ out of 102 samples), diploptene is the dominant hopanoid in over 90 % of hydrocarbon samples (average $f_{\text{diploptene}}$ values 0.64 ± 0.28), even in acidic mineral soils. When compared to peats (average $f_{\text{diploptene}}$ values 0.11 ± 0.11), mineral soils exhibit relatively high $f_{\text{diploptene}}$ values (Fig. 4a). In our RDA (Fig. 1b), MAT and $\delta^{13}\text{C}$ explain 94 % and 93 % of the variation in diploptene, respectively suggesting that diploptene is relatively more abundant in soils with higher $\delta^{13}\text{C}$ values and lower MAT.

The diversity of biohopanoid degradation products (e.g. hopanes, hopenes) in mineral soil is similarly poorly constrained (Ries-Kautt and Albrecht, 1989; Shunthirasingham and Simpson, 2006). Here we detect various diploptene degradation products in our mineral soil samples, including hop-21(22)-ene, hop-17(21)-ene, and neohop-13(18)-ene. The environmental distribution of hop-17(21)-ene and neohop-13(18)-ene is distinct, with both compounds enriched in Brazilian soils (Fig. 1a). The diagenetic transformation of hop-22(29)-ene to neohop-13(18)-ene is well documented (Sinninghe Damsté et al., 2014) and previous studies suggest that the presence of the clay mineral montmorillonite (Ensminger, 1977; Moldovan et al., 1991) and/or strongly acidic conditions (Berti and Bottari, 1968) enhance this diagenetic process (see section 4.2).

We also detect a suite of other C₂₇–C₃₀ hopanes and hopenes in soil, consistent with previous studies (Shunthirasingham and Simpson, 2006). However, the C₃₁ hopane

is rarely detected in our global set of mineral soils and when present only comprises ~2–3 % of the total hopane and hopene assemblage. This contrasts with peats, where the C₃₁ hopane is typically the dominant compound and comprises >30 % of the entire hopane and hopene assemblage (Inglis et al., 2018). In mineral soils with detectable hopanoids ($n = 51$ out of 102 samples), hopanes and hopenes typically occur as the biological ββ isomer, while the thermally mature αβ and βα isomers are a minor constituent of the mineral soil hopanoid assemblage (average: ~5 % of hopanoid assemblage). This is consistent with the few available studies that detected few αβ and βα isomers compared to ββ isomers in mineral soils (Ries-Kautt and Albrecht, 1989; Shunthirasingham and Simpson, 2006) and demonstrates that this is a global phenomenon that is persistent across continents, climate zones, and soil types.

4.2 No relationship between hopane isomerisation and pH in mineral soils

The dominance of the C₃₁ αβ hopane in modern peats has been attributed to acid-catalysed isomerisation of the ββ isomer (Quirk et al., 1984) and there is a significant positive correlation between C₃₁ hopane isomerisation and pH ($r^2 = 0.64$, $p < 0.001$) in a global wetland database (Inglis et al., 2018). Here we assess whether a similar relationship exists between the C₃₁ hopane ββ/(αβ + ββ) index and pH in our global dataset of mineral soils.

In mineral soils, there is no statistically significant linear relationship between the C₃₁ hopane ββ/(αβ + ββ) index and pH ($r = 0.02$, $p = 0.27$; Figure S1 in the Supplementary Material) and redundancy analysis shows that pH only explains 29 % of the variance in the C₃₁ αβ hopane (Fig. 1b). We explored whether MAT and TOC content are correlated with the C₃₁ hopane ββ/(αβ + ββ) index. However, our results indicate no significant linear relationship with TOC ($r = 0.15$, $p = 0.39$) or MAT ($r = 0.08$, $p = 0.65$; Figure S1). As the C₃₁ αβ hopane is rarely detected in mineral soils, we performed the same analysis using a variant of the ββ/(αβ + ββ) index that incorporates all other chain lengths (i.e. C₂₇ to C₃₁). This also indicates no significant relationship between hopane isomerisation and soil pH ($r = 0.16$, $p = 0.26$), TOC content ($r = 0.06$, $p = 0.67$), or MAT ($r = 0.09$, $p = 0.51$) in mineral soils (Fig. S1).

When classified into different pH ranges, very acidic (pH 3 to 5) and moderately acidic (pH 5 to 7) peats have lower ββ/(αβ + ββ) ratios when compared to mineral soils from the same pH range (Fig. 5). For each pH range, C₃₁ ββ/(αβ + ββ) ratios in peat and mineral soil are statistically different ($p < 0.001$; Mann-Whitney U-test). The C₃₁ hopane is relatively common in acidic mineral soils when compared to near neutral-to-alkaline mineral soils (i.e. pH > 6). However, acidic mineral soils exhibit relatively high C₃₁ ββ/(αβ + ββ) ratios compared to acidic peats. The low abundance of αβ hopanes in acidic mineral soils (Fig. 2 and 5) challenges the long-held assumption (Inglis et al., 2018; Pancost et al., 2003; Quirk et al., 1984) that C₃₁ αβ hopanes are acid-catalysed degradation

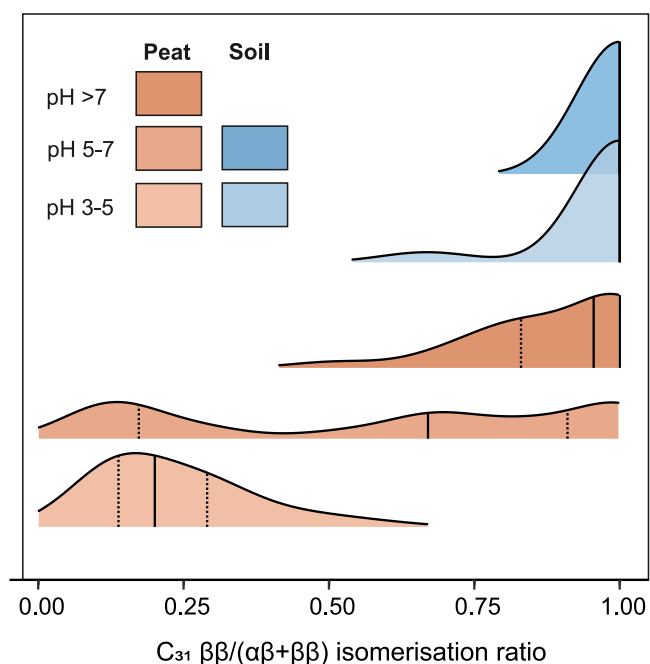


Figure 5. Comparison of C_{31} hopane $\beta\beta/(\alpha\beta + \beta\beta)$ index in mineral soils (Bolivia, Brazil, Colombia, upland Tanzania, Austria and China; this study) and peats (see Inglis et al., 2018). Solid line denotes median value. Dashed lines denote lower and upper quartile.

products that form at low pH and instead, implies that other mechanisms are important (see section 4.3).

Low pH could promote the diagenetic transformation of other hopanoids. For example, the diagenetic transformation of diploptene (hop-22(29)-ene) to neohop-13(18)-ene appears to be enhanced in controlled experiments at low pH (Berti and Bottari, 1968). Consistent with this observation, we only identify neohop-13(18)-ene in mineral soils where $\text{pH} < 5$. However, not all acidic soils contain neohop-13(18)-ene (Fig. S2) and as a result, there is a weak relationship between pH and the ratio between hop-22(29)-ene to neohop-13(18)-ene in mineral soils ($r = 0.29$; Figure S2). This implies that additional mechanisms – such as the presence of clay minerals (Ensminger, 1977; Sinninghe Damsté et al., 2014) – may enhance the diagenetic transformation of diploptene in mineral soils.

4.3 Peats and mineral soils exhibit distinct hopanoid fingerprints

PCA demonstrates that peat and mineral soils are distinctly clustered (Fig. 2a) – this clustering is due to differences in the relative abundance of C_{30} hopenes (e.g. diploptene, moretene, hop-17(21)-ene) vs C_{31} hopanes (Fig. 2a). The C_{31} $\alpha\beta$ hopane has a very strong loading on RDA1 (Fig. 2b) and is negatively correlated with matrix type (i.e. peat vs mineral soil), suggesting that biotic or abiotic processes specific to the depositional environment drive the observed clustering. De novo synthesis of $\alpha\beta$ -BHPs in peat could explain differing hopanoid distributions in peat vs mineral soils. However, only one N_2 -fixing soil bacterium (*Frankia*

spp.) is known to synthesise $\alpha\beta$ -BHPs de novo (Rosa-Putra et al., 2001) and this organism is rarely detected in most peats (Arveby and Huss-Danell, 1988). De novo synthesis of $\alpha\beta$ hopanes is also unlikely given that all known BHPs in peats or mineral soil occur as a single $17\beta,21\beta(\text{H})$ isomer (Talbot et al., 2016). This holds true for early diagenetic intermediates such as tetrakisomohopane-32,33,34-triol and trishomohopane-32,33-diol (e.g. Rodier et al., 1999; Watson and Farrimond, 2000). Rather, isomerisation of the C_{31} hopane appears to occur during or after decarboxylation of the C_{32} hopanoic acid (Inglis et al., 2018; Moldowan et al., 1991). Collectively, this suggests that $\alpha\beta$ hopanes are not inherited from an original biological source organism.

Peats and mineral soils are characterised by different microbial communities (Ausec et al., 2009) and thus, could be characterised by different BHP distributions. Previous studies show that most heterotrophs synthesise BHT and various composite BHPs, with BHT cyclitol ether being the most commonly occurring structure (Talbot et al., 2016; Talbot and Farrimond, 2007). In contrast, methanotrophic bacteria produce non-composite BHPs (i.e. those containing a simple functional group at the C-35 position), with most Type I methanotrophs producing aminopentol and aminotetrol and most Type II species producing BHT, aminotetrol and aminotriol (although we note that aminotriol can also have a non-methanotrophic origin; Talbot et al., 2016). Despite differences in BHP diversity between microbial groups, globally-distributed peats and mineral soils are generally characterised by a similar suite of BHPs and are dominated by three tetrafunctionalised BHPs (BHT, BHT-cyclitol ether, and aminotriol). This suggests that heterotrophic bacteria are the main hopanoid-producing organisms in mineral soils and peat (Spencer-Jones et al., 2015; Talbot et al., 2016). Thus, differences in bacterial community composition between mineral soils and peat are unlikely to exert a first order control on BHP distributions and thus, their degradation products. Mineral soils typically contain a lower abundance of BHPs than peat deposits (Spencer-Jones et al., 2015), implying that the concentration of BHP-degradation products (e.g. hopanes) will be lower in mineral soils than in peats. This may explain why the C_{31} hopane is rarely detected in our mineral soil dataset (Fig. 3). However, this would not be expected to impact $\beta\beta/(\alpha\beta + \beta\beta)$ ratios and it does not explain why acidic mineral soils lack $\alpha\beta$ hopanes when compared to acidic peats.

Instead, we argue that the relative abundance of different organic carbon pools in peat vs mineral soils acts to selectively protect BHPs from degradation and subsequent isomerisation. Peat is dominated by particulate organic carbon (POC) and contains relatively few clay minerals. As such, bacterial biomass is highly vulnerable to microbial decomposition in the oxic acrotelm (i.e. the top 15–30 cm; Loisel et al., 2021). In contrast, mineral soils are characterised by a mixture of POC and mineral-associated organic carbon (MAOC). The latter may comprise up to 70 % of soil organic carbon (Georgiou et al., 2022) and has been shown to play a key role in stabilising microbial necromass (Angst et al., 2021; Gies et al., 2021) over longer timescales

(decades to millennia). We propose that a large fraction of BHPs preserved in mineral soils are protected from degradation, which inhibits the formation of C₃₂ hopanoic acids and C₃₁ hopanes. As isomerisation of the C₃₁ hopane occurs during or after decarboxylation of the C₃₂ hopanoic acid, this may explain the low abundance of αβ hopanes in (acidic) mineral soils. Coupled analysis of hopanoids and mineral surface area in downcore mineral soil profiles would help to directly test this hypothesis. Beyond mineral protection, other abiotic (e.g. temperature) and biotic (e.g. microbial community, total organic carbon content) variables may be important and require further study.

4.4 Using hopane isomerisation ratios as paleo-environmental proxies

In mineral soils, there is no relationship between pH and hopane isomerisation ratios (see section 4.2) and we do not recommend using hopane ββ/(αβ + ββ) ratios to infer pH in ancient soil (paleosol) deposits. In peat, there is an empirical relationship between pH and the C₃₁ hopane ββ/(αβ + ββ) ratio (Inglis et al., 2018; this study) and this proxy can be used to reconstruct pH in modern and ancient peat-forming environments (e.g. Schaaff et al., 2024). Given that different hopane chain lengths should be similarly affected by changes in pH, past findings imply that other hopanes (e.g. C₂₉ or C₃₀) could also be used to reconstruct past pH variations. However, recent work has shown opposing variations in the C₃₁ and C₃₀ ββ/(αβ + ββ) ratio in a Holocene-aged wetland (Schaaff et al., 2024). To explore this further, we re-examined the empirical relationship between (i) pH and the ≤ C₃₀ hopane ββ/(αβ + ββ) index and (ii) pH and the C₃₁ hopane ββ/(αβ + ββ) index in our reduced global peat database (n = 24). Intriguingly, we find no significant relationship between ≤ C₃₀ hopane ββ/(αβ + ββ) ratio and pH (r² = 0.10, p = 0.24) in modern peats (Fig. S3), suggesting that only the C₃₁ hopane ββ/(αβ + ββ) index can be used to infer pH in peat-forming environments.

We suggest this is because C₃₀ and C₃₁ hopanes undergo different diagenetic pathways in peat. C₃₁ hopanes form via BHPs that undergo a series of oxidation and decarboxylation reactions (Inglis et al., 2018; Synnott et al., 2021). Oxidation and decarboxylation reactions will typically favour the production of more reactive intermediates, such as free radicals, carbocations or carboanions, which can potentially promote changes in hopane stereochemistry. ≤ C₃₀ hopanes can form via side chain cleavage of the C₃₁ hopane but can also form via reduction of diploptene and/or diplopterol (Synnott et al., 2021). Reduction reactions typically involve the addition of electrons or hydrogen atoms, which would typically stabilise the molecule and reduce the likelihood of isomerization. Further work is required to explore this, but differences in diagenetic pathways may explain why C₃₁ and ≤ C₃₀ hopane ββ/(αβ + ββ) ratio have a different relationship with pH in peat.

Thermally mature hopanes are detectable in a range of modern environments, including mineral soils and peat. As these environments have not undergone thermal maturation, we suggest that future studies describe these compounds

as thermodynamically stable (rather than thermally mature). Although αβ hopanes are detectable in soils (see sections 4.1 and 4.2) they are far less abundant than in acidic peats (Fig. 1). Thus, we propose that low hopane isomerisation ratios could help fingerprint the delivery of (acidic) peat into the marine realm. Indeed, previous studies have identified low C₃₁ hopane ββ/(αβ + ββ) ratios in recent (last 400 years) marine sediment cores and suggested this represents the input of peat organic matter (Smittenberg et al., 2004). Similarly, in a thermally-immature early Eocene (ca. 53 to 51 million years old) marine sediment core from offshore Antarctica, there is an unusually high abundance of the thermodynamically stable C₃₁ αβ hopane isomer within an otherwise immature hopane assemblage (Inglis et al., 2022). These sediments exhibit relatively low C₃₁ hopane ββ/(αβ + ββ) ratios 0.4–0.7; (Inglis et al., 2022) and imply input of peat organic matter into the marine realm. The additional presence of *Sphagnum* moss spores in these sediments (Contreras et al., 2013) supports the input and incorporation of peat-derived organic matter into the marine environment. We suggest this approach could build upon other biomarker-based proxies developed to trace the input of soil-derived OC into the marine realm (e.g. the BIT index; C/N ratios; Hopmans et al., 2004; Weijers et al., 2009). This approach has the advantage of being able to differentiate between peat vs soil organic carbon. The approach is also particularly powerful given that *Sphagnum* spores (used to infer peat input) are relatively rare or absent in marine sediments due to taphonomic processes (see Inglis et al., 2015 and references therein) and not all peatlands are dominated by *Sphagnum*. Changes in the abundance of C₃₁ αβ hopane in marine sediments could reveal changes in wetland extent over geological time, but only if marine sediments have undergone minimal thermal maturation. However, a full characterisation of hopanoid distributions in modern marine environments is required to determine the feasibility of this approach.

5 Conclusion

Hopane isomerisation ratios are used to reconstruct pH in ancient peat-forming environments. However, it is unclear whether this approach is transferable to mineral soils. To explore this further, we analysed hopane distributions in a wide range of modern mineral soils and evaluated the relationship between hopane distribution and isomerisation ratios with different environmental variables. We demonstrate that peats and mineral soils are characterised by distinct hopane distributions. As heterotrophic bacteria are the primary hopanoid-producing organisms in both environments, changes in the bacterial community are unlikely to explain this difference. Instead, we propose that the high abundance of (clay) minerals in mineral soils (compared to peat) may protect BHPs from degradation and subsequent isomerisation. Unlike peats, there is no relationship between hopane isomerisation and pH in soil. This implies that hopane isomerisation ratios are not applicable as quantitative pH proxies in mineral soil environments. However,

we suggest that diagnostic hopanes (specifically the C₃₁ αβ hopane) could provide insights into the mobilisation and delivery of peat organic matter into the marine realm and may have the potential to reveal changes in peatland extent in the geological record but requires further proxy validation.

6 Acknowledgements

GNI is supported by a GCRF Royal Society Dorothy Hodgkin Fellowship (DHF\R1\191178) with additional support via the Royal Society (RF\ERE\231019, RF\ERE\210068). CH and the sample collection of Brazilian soils were supported by a Swiss National Science Foundation (SNF) mobility fellowship (Grant P400P2_183856). DJB acknowledges the financial support from FAPESP (2022/06440-1). TKA acknowledges the financial support from FAPESP (2019/19948-0 and 2021/13129-8) and CAPES/Cofecub (88887.989386/2024-00). BDAN acknowledges funding through a Royal Society Tata University Research Fellowship. Soils from Austria, Bolivia, China and Tanzania are collected through the regional Technical Cooperation Project INT5153, from the International Atomic Energy Agency (IAEA). We thank Marco Griepentrog, Andreas Richter, Edson Ramirez, Xinbao Zhang, Pascal Boeckx for coordinating the collection of these samples. The Serengeti sampling was supported with funds from the National Science Foundation [EAR-PF grant #1725621] to EB. Samples were collected under permits issued to EB by the Tanzanian government under COSTECH Permit #2018-39-NA-2018-17, TANAPA Research Permit #: TNP/HQ/C.10/13, and TAWIRI Permit #: TWRI/RS-342/2016/116. Thanks to Joseph Masoy and Honest Ndoro for field assistance and Yannick Matia and Efrain Vidal for laboratory assistance with sample preparation, supported with funds from the University of Southern California. Finally, we thank Jessica Tierney, Stephanie Kusch, Darci Rush, and one anonymous reviewer for the constructive feedback that has substantially improved this manuscript.

Data, code, and outputs availability statement

The processed data used in this study are available at OSF (<https://doi.org/10.17605/OSF.IO/3CNJZ>; Inglis, 2025) and associated with a CC-BY Attribution 4.0 International licence.

Licence agreement

This article is distributed under the terms of the Creative Commons Attribution 4.0 International Licence (CC BY 4.0), which permits unrestricted use, distribution, and reproduction in any medium, provided appropriate credit is given to the original author(s) and source, as well as a link to the Creative Commons licence, and an indication of changes that were made.

References

- Aitchison J (1986). *The Statistical Analysis of Compositional Data*. Springer Netherlands. doi:10.1007/978-94-009-4109-0.
- Angst G, Mueller KE, Nierop KG, Simpson MJ (2021). Plant- or microbial-derived? A review on the molecular composition of stabilized soil organic matter. *Soil Biology and Biochemistry* 156: 108189. doi:10.1016/j.soilbio.2021.108189.
- Arveby A, Huss-Danell K (1988). Presence and dispersal of infective Frankia in peat and meadow soils in Sweden. *Biology and Fertility of Soils* 6(1). doi:10.1007/bf00257918.
- Ausec L, Kraigher B, Mandic-Mulec I (2009). Differences in the activity and bacterial community structure of drained grassland and forest peat soils. *Soil Biology and Biochemistry* 41(9): 1874–1881. doi:10.1016/j.soilbio.2009.06.010.
- Berti G, Bottari F (1968). Constituents of ferns. In Reinhold L, Livschitz Y (eds.) *Progress in phytochemistry*, vol. 1, pp. 589–685. Interscience, London.
- Beverly EJ, Levin NE, Passey BH, Aron PG, Yarian DA, Page M, Pelletier EM (2021). Triple oxygen and clumped isotopes in modern soil carbonate along an aridity gradient in the Serengeti, Tanzania. *Earth and Planetary Science Letters* 567: 116952. doi:10.1016/j.epsl.2021.116952.
- van den Boogaart KG, Tolosana-Delgado R (2008). "Compositions": A unified R package to analyze compositional data. *Computers & Geosciences* 34(4): 320–338. doi:10.1016/j.cageo.2006.11.017.
- Bradley AS, Pearson A, Sáenz JP, Marx CJ (2010). Adenosylhopane: The first intermediate in hopanoid side chain biosynthesis. *Organic Geochemistry* 41(10): 1075–1081. doi:10.1016/j.orggeochem.2010.07.003.
- Brady N, Weil R (2008). *The nature and properties of soils*. Prentice Hall, Upper Saddle River, NJ, 14 edn.
- Contreras L, Pross J, Bijl PK, Koutsodendris A, Raine JL, van de Schootbrugge B, Brinkhuis H (2013). Early to Middle Eocene vegetation dynamics at the Wilkes Land Margin (Antarctica). *Review of Palaeobotany and Palynology* 197: 119–142. doi:10.1016/j.revpalbo.2013.05.009.
- De Jonge C, Guo J, Hållberg P, Griepentrog M, Rifai H, Richter A, Ramirez E, Zhang X, Smittenberg RH, Peterse F, Boeckx P, Dercon G (2024). The impact of soil chemistry, moisture and temperature on branched and isoprenoid GDGTs in soils: A study using six globally distributed elevation transects. *Organic Geochemistry* 187: 104706. doi:10.1016/j.orggeochem.2023.104706.
- Ensminger A (1977). *Evolution de composés polycycliques sédimentaires*. L'Université Louis Pasteur de Strasbourg.
- Farrimond P, Taylor A, Telnæs N (1998). Biomarker maturity parameters: the role of generation and thermal degradation. *Organic Geochemistry* 29(5–7): 1181–1197. doi:10.1016/s0146-6380(98)00079-5.
- Georgiou K, Jackson RB, Vindušková O, Abramoff RZ, Ahlström A, Feng W, Harden JW, Pellegrini AFA, Polley HW, Soong JL, Riley WJ, Torn MS (2022). Global stocks and capacity of mineral-associated soil organic carbon. *Nature Communications* 13(1). doi:10.1038/s41467-022-31540-9.
- Gies H, Hagedorn F, Lupker M, Montluçon D, Haghipour N, van der Voort TS, Eglinton TI (2021). Millennial-age glycerol dialkyl glycerol tetraethers (GDGTs) in forested mineral soils: ¹⁴C-based evidence for stabilization of microbial necromass. *Biogeosciences* 18(1): 189–205. doi:10.5194/bg-18-189-2021.

- Hopmans EC, Weijers JW, Schefuß E, Herfort L, Sinninghe Damsté JS, Schouten S (2004). A novel proxy for terrestrial organic matter in sediments based on branched and isoprenoid tetraether lipids. *Earth and Planetary Science Letters* 224(1–2): 107–116. doi:10.1016/j.epsl.2004.05.012.
- Huang X, Meyers PA, Xue J, Gong L, Wang X, Xie S (2015). Environmental factors affecting the low temperature isomerization of homohopanes in acidic peat deposits, central China. *Geochimica et Cosmochimica Acta* 154: 212–228. doi:10.1016/j.gca.2015.01.031.
- Häggi C, Bertassoli DJ, Akabane TK, So RT, Sawakuchi AO, Chiessi CM, Mendes VR, Jaramillo CA, Feakins SJ (2024). Using Multi-Homolog Plant-Wax Carbon Isotope Compositions to Reconstruct Tropical Vegetation Types. *Journal of Geophysical Research: Biogeosciences* 129(4). doi:10.1029/2023jg007946.
- Häggi C, Naafs BDA, Silvestro D, Bertassoli DJ, Akabane TK, Mendes VR, Sawakuchi AO, Chiessi CM, Jaramillo CA, Feakins SJ (2023). GDGT distribution in tropical soils and its potential as a terrestrial paleothermometer revealed by Bayesian deep-learning models. *Geochimica et Cosmochimica Acta* 362: 41–64. doi:10.1016/j.gca.2023.09.014.
- Inglis GN (2025). Hopanoid distributions differ in mineral soils and peat: a re-evaluation of hopane-based pH proxies. doi:10.17605/OSF.IO/3CNJZ.
- Inglis GN, Collinson ME, Riegel W, Wilde V, Robson BE, Lenz OK, Pancost RD (2015). Ecological and biogeochemical change in an early Paleogene peat-forming environment: Linking biomarkers and palynology. *Palaeogeography, Palaeoclimatology, Palaeoecology* 438: 245–255. doi:10.1016/j.palaeo.2015.08.001.
- Inglis GN, Farnsworth A, Collinson ME, Carmichael MJ, Naafs BDA, Lunt DJ, Valdes PJ, Pancost RD (2019). Terrestrial environmental change across the onset of the PETM and the associated impact on biomarker proxies: A cautionary tale. *Global and Planetary Change* 181: 102991. doi:10.1016/j.gloplacha.2019.102991.
- Inglis GN, Naafs BDA, Zheng Y, McClymont EL, Evershed RP, Pancost RD (2018). Distributions of geohopanooids in peat: Implications for the use of hopanoid-based proxies in natural archives. *Geochimica et Cosmochimica Acta* 224: 249–261. doi:10.1016/j.gca.2017.12.029.
- Inglis GN, Toney JL, Zhu J, Poulsen CJ, Röhl U, Jamieson SSR, Pross J, Cramwinckel MJ, Krishnan S, Pagani M, Bijl PK, Bendle J (2022). Enhanced Terrestrial Carbon Export From East Antarctica During the Early Eocene. *Paleoceanography and Paleoclimatology* 37(2). doi:10.1029/2021pa004348.
- Kusch S, Rush D (2022). Revisiting the precursors of the most abundant natural products on Earth: A look back at 30+ years of bacteriohopanepolyol (BHP) research and ahead to new frontiers. *Organic Geochemistry* 172: 104469. doi:10.1016/j.orggeochem.2022.104469.
- Lauretano V, Kennedy-Asser AT, Korasidis VA, Wallace MW, Valdes PJ, Lunt DJ, Pancost RD, Naafs BDA (2021). Eocene to Oligocene terrestrial Southern Hemisphere cooling caused by declining pCO₂. *Nature Geoscience* 14(9): 659–664. doi:10.1038/s41561-021-00788-z.
- Loisel J, Gallego-Sala AV, Amesbury MJ, Magnan G, Anshari G, Beilman DW, Benavides JC, Blewett J, Camill P, Charman DJ, Chawchai S, Hedgpeth A, Kleinen T, Korhola A, Large D, Mansilla CA, Müller J, van Bellen S, West JB, Yu Z, Bubier JL, Garneau M, Moore T, Sannel ABK, Page S, Välranta M, Bechtold M, Brovkin V, Cole LES, Chanton JP, Christensen TR, Davies MA, De Vleeschouwer F, Finkelstein SA, Frolking S, Gałka M, Gandois L, Girkin N, Harris LI, Heinemeyer A, Hoyt AM, Jones MC, Joos F, Juutinen S, Kaiser K, Lacourse T, Lamentowicz M, Larmola T, Leifeld J, Lohila A, Milner AM, Minkinen K, Moss P, Naafs BDA, Nichols J, O'Donnell J, Payne R, Philben M, Piilo S, Quillet A, Ratnayake AS, Roland TP, Sjögersten S, Sonnentag O, Swindles GT, Swinnen W, Talbot J, Treat C, Valach AC, Wu J (2021). Expert assessment of future vulnerability of the global peatland carbon sink. *Nature Climate Change* 11(1): 70–77. doi:10.1038/s41558-020-00944-0.
- Mackenzie A, Patience R, Maxwell J, Vandenbroucke M, Durand B (1980). Molecular parameters of maturation in the Toarcian shales, Paris Basin, France—I. Changes in the configurations of acyclic isoprenoid alkanes, steranes and triterpanes. *Geochimica et Cosmochimica Acta* 44(11): 1709–1721. doi:10.1016/0016-7037(80)90222-7.
- Moldowan J, Fago FJ, Carlson RM, Young DC, an Duvne G, Clardy J, Schoell M, Pillinger CT, Watt DS (1991). Rearranged hopanes in sediments and petroleum. *Geochimica et Cosmochimica Acta* 55(11): 3333–3353. doi:10.1016/0016-7037(91)90492-n.
- Naafs B, Inglis G, Zheng Y, Amesbury M, Biester H, Bindler R, Blewett J, Burrows M, del Castillo Torres D, Chambers F, Cohen A, Evershed R, Feakins S, Gałka M, Gallego-Sala A, Gandois L, Gray D, Hatcher P, Honorio Coronado E, Hughes P, Huguet A, Könönen M, Laggoun-Défarge F, Lääteenoja O, Lamentowicz M, Marchant R, McClymont E, Pontevedra-Pombal X, Ponton C, Pourmand A, Rizzuti A, Rochefort L, Schellekens J, De Vleeschouwer F, Pancost R (2017). Introducing global peat-specific temperature and pH calibrations based on brGDGT bacterial lipids. *Geochimica et Cosmochimica Acta* 208: 285–301. doi:10.1016/j.gca.2017.01.038.
- Oksanen J, Simpson GL, Blanchet FG, Kindt R, Legendre P, Minchin PR, O'Hara R, Solymos P, Stevens MHH, Szoecs E, Wagner H, Barbour M, Bedward M, Bolker B, Borcard D, Borman T, Carvalho G, Chirico M, De Caceres M, Durand S, Evangelista HBA, FitzJohn R, Friendly M, Furneaux B, Hannigan G, Hill MO, Lahti L, Martino C, McGlinn D, Ouellette MH, Ribeiro Cunha E, Smith T, Stier A, Ter Braak CJ, Weedon J (2001). vegan: Community Ecology Package. doi:10.32614/cran.package.vegan.
- Ourisson G, Albrecht P (1992). Hopanooids. 1. Geohopanooids: the most abundant natural products on Earth? *Accounts of Chemical Research* 25(9): 398–402. doi:10.1021/ar00021a003.
- Pancost RD, Baas M, van Geel B, Sinninghe Damsté JS (2003). Response of an ombrotrophic bog to a regional climate event revealed by macrofossil, molecular and carbon isotopic data. *The Holocene* 13(6): 921–932. doi:10.1191/0959683603hl674rp.
- Peaple MD, Beverly EJ, Garza B, Baker S, Levin NE, Tierney JE, Häggi C, Feakins SJ (2022). Identifying the drivers of GDGT distributions in alkaline soil profiles within the Serengeti ecosystem. *Organic Geochemistry* 169: 104433. doi:10.1016/j.orggeochem.2022.104433.
- Quirk M, Wardroper A, Wheatley R, Maxwell J (1984). Extended hopanooids in peat environments. *Chemical Geology* 42(1–4): 25–43. doi:10.1016/0009-2541(84)90003-2.
- Ries-Kautt M, Albrecht P (1989). Hopane-derived triterpenoids in soils. *Chemical Geology* 76(1–2): 143–151. doi:10.1016/0009-2541(89)90133-2.
- Robinson SA, Ruhl M, Astley DL, Naafs BDA, Farnsworth AJ, Bown PR, Jenkyns HC, Lunt DJ, O'Brien C, Pancost RD, Markwick PJ (2017). Early Jurassic North Atlantic sea-surface temperatures from TEX86 palaeothermometry. *Sedimentology* 64(1): 215–230. doi:10.1111/sed.12321.
- Rodier C, Llopiz P, Neunlist S (1999). C₃₂ and C₃₄ hopanooids in recent sediments of European lakes: novel intermediates in the early diagenesis of biohopanooids. *Organic Geochemistry* 30(7): 713–716. doi:10.1016/S0146-6380(99)00045-5.
- Rohmer M, Bouvier-Nave P, Ourisson G (1984). Distribution of Hopanoid Triterpenes in Prokaryotes. *Microbiology* 130(5): 1137–1150. doi:10.1099/00221287-130-5-1137.

- Rosa-Putra S, Nalin R, Domenach A, Rohmer M (2001). Novel hopanoids from *Frankia* spp. and related soil bacteria: Squalene cyclization and significance of geological biomarkers revisited. *European Journal of Biochemistry* 268(15): 4300–4306. doi:10.1046/j.1432-1327.2001.02348.x.
- Schaaff V, Grossi V, Makou M, Garcin Y, Deschamps P, Sebag D, Ngounou Ngatcha B, Ménot G (2024). Constraints on hopanes and brGDGTs as pH proxies in peat. *Geochimica et Cosmochimica Acta* 373: 342–354. doi:10.1016/j.gca.2024.03.034.
- Sessions AL, Zhang L, Welander PV, Doughty D, Summons RE, Newman DK (2013). Identification and quantification of polyfunctionalized hopanoids by high temperature gas chromatography–mass spectrometry. *Organic Geochemistry* 56: 120–130. doi:10.1016/j.orggeochem.2012.12.009.
- Shunthirasingham C, Simpson MJ (2006). Investigation of bacterial hopanoid inputs to soils from Western Canada. *Applied Geochemistry* 21(6): 964–976. doi:10.1016/j.apgeochem.2006.03.007.
- Sinninghe Damsté JS, Schouten S, Volkman JK (2014). C₂₇–C₃₀ neohop-13(18)-enes and their saturated and aromatic derivatives in sediments: Indicators for diagenesis and water column stratification. *Geochimica et Cosmochimica Acta* 133: 402–421. doi:10.1016/j.gca.2014.03.008.
- Slowikowski K (2024). ggrepel: Automatically Position Non-Overlapping Text Labels with 'ggplot2'. doi:10.32614/cran.package.ggrepel. R package version 0.9.3.
- Smittenberg R, Pancost R, Hopmans E, Paetzel M, Sinninghe Damsté J (2004). A 400-year record of environmental change in an euxinic fjord as revealed by the sedimentary biomarker record. *Palaeogeography, Palaeoclimatology, Palaeoecology* 202(3–4): 331–351. doi:10.1016/s0031-0182(03)00642-4.
- Spencer-Jones CL, Wagner T, Dinga BJ, Schefuß E, Mann PJ, Poulsen JR, Spencer RG, Wabakanghanzi JN, Talbot HM (2015). Bacteriohopanepolyols in tropical soils and sediments from the Congo River catchment area. *Organic Geochemistry* 89–90: 1–13. doi:10.1016/j.orggeochem.2015.09.003.
- Synnott DP, Schwark L, Dewing K, Percy EL, Pedersen PK (2021). The diagenetic continuum of hopanoid hydrocarbon transformation from early diagenesis into the oil window. *Geochimica et Cosmochimica Acta* 308: 136–156. doi:10.1016/j.gca.2021.06.005.
- Sáenz JP, Grosser D, Bradley AS, Lagny TJ, Lavrynenko O, Broda M, Simons K (2015). Hopanoids as functional analogues of cholesterol in bacterial membranes. *Proceedings of the National Academy of Sciences* 112(38): 11971–11976. doi:10.1073/pnas.1515607112.
- Talbot HM, Farrimond P (2007). Bacterial populations recorded in diverse sedimentary biohopanoid distributions. *Organic Geochemistry* 38(8): 1212–1225. doi:10.1016/j.orggeochem.2007.04.006.
- Talbot HM, McClymont EL, Inglis GN, Evershed RP, Pancost RD (2016). Origin and preservation of bacteriohopanepolyol signatures in Sphagnum peat from Bissendorfer Moor (Germany). *Organic Geochemistry* 97: 95–110. doi:10.1016/j.orggeochem.2016.04.011.
- Watson D, Farrimond P (2000). Novel polyfunctionalised geohopaneoids in a recent lacustrine sediment (Priest Pot, UK). *Organic Geochemistry* 31(11): 1247–1252. doi:10.1016/S0146-6380(00)00148-0.
- Weijers JW, Schouten S, Schefuß E, Schneider RR, Sinninghe Damsté JS (2009). Disentangling marine, soil and plant organic carbon contributions to continental margin sediments: A multi-proxy approach in a 20,000 year sediment record from the Congo deep-sea fan. *Geochimica et Cosmochimica Acta* 73(1): 119–132. doi:10.1016/j.gca.2008.10.016.
- Wickham H, Chung W, Girlich M (2019). scales: Scale Functions for Visualization. doi:10.32614/cran.package.scales. R package version 1.2.1.
- Wickham H, François R, Henry L, Müller K, Vaughan D (2023). dplyr: A Grammar of Data Manipulation. doi:10.32614/CRAN.package.dplyr. R package version 1.1.3.
- Wilke CO (2017). ggrridges: Ridgeline Plots in "ggplot2". doi:10.32614/cran.package.ggrridges.
- Witkowski CR, Lauretano V, Farnsworth A, Li S, Li SH, Mayser JP, Naafs BDA, Spicer RA, Su T, Tang H, Zhou ZK, Valdes PJ, Pancost RD (2023). Dynamic environment but no temperature change since the late Paleogene at Lühe Basin (Yunnan, China). *EGUsphere preprint repository* doi:10.5194/egusphere-2023-373.
- Zhang D, Beverly EJ, Levin NE, Vidal E, Matia Y, Feakins SJ (2021). Carbon isotopic composition of plant waxes, bulk organics and carbonates from soils of the Serengeti grasslands. *Geochimica et Cosmochimica Acta* 311: 316–331. doi:10.1016/j.gca.2021.07.005.